

Electronic structure and magnetism in doped semiconducting half-Heusler compounds

B.R.K. Nanda and I. Dasgupta[§]

Department of Physics, Indian Institute of Technology Bombay, Powai, Mumbai 400076, India

Abstract. We have studied in details the electronic structure and magnetism in M (Mn and Cr) doped semiconducting half-Heusler compounds FeVSb, CoTiSb and NiTiSn ($\text{XM}_x\text{Y}_{1-x}\text{Z}$) in a wide concentration range using local-spin density functional method in the framework of tight-binding linearized muffin tin orbital method(TB-LMTO) and supercell approach. Our calculations indicate that some of these compounds are not only ferromagnetic but also half-metallic and may be useful for spintronics applications. The electronic structure of the doped systems is analyzed with the aid of a simple model where we have considered the interaction between the dopant transition metal (M) and the valence band X-Z hybrid. We have shown that the strong X-d - M-d interaction places the M-d states close to the Fermi level with the M- t_{2g} states lying higher in energy in comparison to the M- e_g states. Depending on the number of available d-electrons, ferromagnetism is realized provided the d-manifold is partially occupied. The tendencies toward ferromagnetic(FM) or antiferromagnetic(AFM) behavior are discussed within Anderson-Hasegawa models of super-exchange and double-exchange. In our calculations for Mn doped NiTiSn, the strong preference for FM over AFM ordering suggests a possible high Curie temperature for these systems.

[§] To whom correspondence should be addressed (dasgupta@phy.iitb.ac.in)

1. Introduction

Spin-based electronics or spintronics is currently an active area of research because it provides a possibility to integrate electronic, opto-electronic and magneto-electronic multifunctionality on a single device exploiting both spin as well as charge degree of freedom of an electron. The half-metallic ferromagnets having only one electronic spin direction at the Fermi energy resulting in 100% spin-polarization and ferromagnetic semiconductors where magnetic and semiconducting properties can be controlled and tuned are suggested to be suitable candidates for spintronic applications. The recent interest in ferromagnetic semiconductors for spintronic applications is spurred by the pioneering work by Ohno and co-workers[1], in the late nineties, showing that a ferromagnetic Curie temperature as high as 110 K can be achieved in Mn doped GaAs, demonstrating the feasibility that ferromagnetic property can be incorporated in traditional semiconductors. This work has stimulated vigorous experimental as well as theoretical activity in diluted magnetic semiconductors (DMSs). As a result, on the experimental front, ferromagnetism in diluted magnetic semiconductors, in some cases with T_c close to room temperature have been reported for Mn doped GaP[2], Mn-doped Chalcopyrite CdGeP_2 [3] and Mn doped GaN[4, 5]. Ferromagnetism has also been reported for oxide based diluted magnetic semiconductors such as Co doped TiO_2 [6], SnO_2 [7] and $\text{La}_{1-x}\text{Sr}_x\text{TiO}_{3-\delta}$ [8].

The present theoretical understanding of ferromagnetism in DMSs is very limited. The widely accepted model Hamiltonian[9] for Mn-doped DMSs *e.g.* $\text{Ga}_{1-x}\text{Mn}_x\text{Sb}$ considers the impurity state bound to Mn ion to be shallow acceptors formed from the host material and the interaction between the Mn impurity spin orientations to be mediated by valence band holes. The exchange interaction between the localized transition metal impurities and the hole is suggested to be RKKY like, and it has been argued that such a model can capture salient features of the diluted magnetic semiconductors. The other possible mechanism that can stabilize ferromagnetism in DMS is suggested to be Zener's p-d exchange[10]. On the other hand, the first principles calculations suggest that the Mn induced hole can have significant 3-d character. In the series [11] Mn doped $\text{GaN} \rightarrow \text{GaP} \rightarrow \text{GaAs} \rightarrow \text{GaSb}$ the hole generated by introducing Mn in GaN is found to have significant 3d character, while in GaSb the hole is found to have primarily host character. Further the first principles calculations suggest that ferromagnetism is stabilized by kinetic energy driven mechanism either by hybridization induced negative exchange splitting [12] or double exchange[13] depending on the nature and the location of the holes.

The discussion of the preceding paragraph suggests that the mechanism behind ferromagnetism in DMSs is still far from complete. It also raises the important questions whether any transition metal (TM) -semiconductor combination will result in ferromagnetism and what are the relevant energetics that govern the interaction of the transition metal with the host resulting in ferromagnetism. To understand some of these issues the current research effort in spintronics materials is also directed

toward search for potential DMS hosts. Recently it was found experimentally[14] that semiconducting tetradymite structure material Sb_2Te_3 act as DMS with $T_c \simeq 20\text{K}$ when doped with few per cent of V atoms. Similarly a recent, first principles calculation, [15] indicate that transition metal doped SiC may be ferromagnetic with T_c very close to room temperature. In the present work we have considered semiconducting half-Heusler systems as a potential DMS host.

The half-Heusler compounds with the general formula XYZ, where X and Y are transition metals and Z is a sp-valent element has been a subject of continuous attention because of their variety of novel magnetic properties ranging from antiferromagnets[16], half-metallic ferromagnets[17], weak ferromagnets, Pauli metals, semimetals[18] to semiconductors[19]. In particular, the half-metallic semi-Heusler alloys can be attractive for spintronics applications due to their relatively high Curie temperature and similarity of the crystal structure to zinc-blende structure which are adopted by a large number of semiconductors like GaAs, ZnSe, InAs *etc.*. In the present work, inspired by DMSs we have examined in details the electronic structure of 18 valence electron semiconducting half-Heusler alloys FeVSb, CoTiSb and NiTiSn when doped with transition metal impurities Mn and Cr. The electronic structure of Mn doped semiconducting half-Heusler alloys have also been investigated in the framework of KKR-CPA calculations[20]. The doped Heusler systems has also been a subject of interest due to the possibility of realizing half-metallic antiferromagnetism[21] Half-metallic antiferromagnets are half-metallic systems with vanishing macroscopic moment. Our calculations for the doped semi-conducting half-Heusler systems suggests, for impurity concentrations as low as 3 % some semiconducting half-Heusler systems are transformed to half-metallic ferromagnets, with possibly with high Curie temperature.

The rest of the paper is organized as follows. In section 2 we describe the crystal structure and the computational details. A detailed analysis of the electronic structure and magnetism of doped Heusler systems is carried out in section 3. Finally, in section 4 we present our conclusions.

2. Structure and computational details

The half-Heusler compounds XYZ crystallize in the face centered cubic structure with one formula unit per unit cell as shown in figure 1. The space group is $F4/3m$ (No 216). For the semiconducting half-Heusler systems considered here the higher valent transition elements Fe,Co and Ni represent X while the lower valent transition element V, Ti represent Y and Sb/Sn represent Z. In the conventional stable structure Y and Z atoms are located at $4a(0,0,0)$ and $4b(\frac{1}{2},\frac{1}{2},\frac{1}{2})$ positions, forming the rock salt structure arrangement. The X atom is located in the octahedral coordinated pocket, at one of the cube center positions $4c(\frac{1}{4}, \frac{1}{4}, \frac{1}{4})$ leaving the other $4d(\frac{3}{4}, \frac{3}{4}, \frac{3}{4})$ empty. When the Z-atomic positions are empty the structure is analogous to zinc blende structure, which is common for large number of semiconductors.

In order to study the effect of Mn and Cr impurities (M) in semi-conducting half-

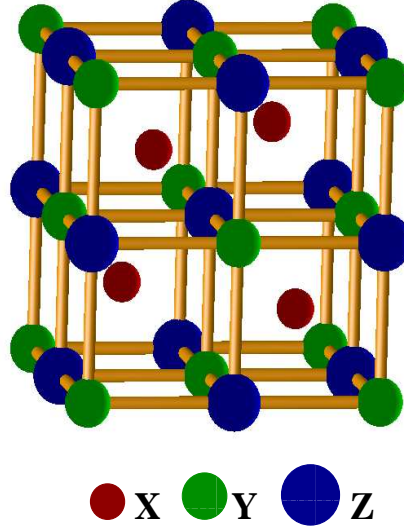


Figure 1. The cubic half-Heusler structure

Heusler systems (*i.e.* to simulate the effect of doping) we have constructed supercells with size dependent on the percent of M doping. In each supercell we have replaced either one or two Y atoms by M atoms. For the two impurities embedded in the supercell we have studied the electronic structure of these doped systems both as a function of orientation of one M atom with respect to the other as well as distance between the two M atoms. Further embedding a pair of impurity atoms also allowed us to study the interaction between a pair of M moments. The largest supercell chosen was 64 times the original unit cell and consisted of 192(256) atoms (including the empty spheres) to simulate 3.125 % concentration for a pair of M atoms. The size of the supercell was chosen to ensure that the separation between the impurities is much smaller in comparison to the dimension of the supercell.

All the electronic structure calculations reported in this work have been performed using self-consistent tight-binding linear muffin-tin orbital (TB-LMTO) method with the atomic sphere approximation (ASA) and the Combined Correction[22]. TB-LMTO-ASA has been established as an intelligible, fast and accurate method to understand electronic structure and chemical bonding for a large case of solids, including systems with pronounced directional bonding[23, 24]. Recently we have employed[25] the TB-LMTO-ASA method coupled with the crystal orbital Hamiltonian population(COHP)[26] for an energy-resolved visualization of chemical bonding in half-Heusler systems. Self-consistent TB-LMTO-ASA calculations are done in the framework of LDA[27]. We have also checked our calculations within generalized gradient approximation (GGA)[28] and the results are found to be very similar to the LDA results. The space filling in the ASA is achieved by inserting empty spheres in the cube center positions $(\frac{3}{4}, \frac{3}{4}, \frac{3}{4})$ and by inflating the atom-centered non-overlapping spheres. The atomic radii are chosen in such a way that there is negligible charge on the empty spheres and the overlap of the interstitial with the interstitial, atomic with atomic and interstitial with the

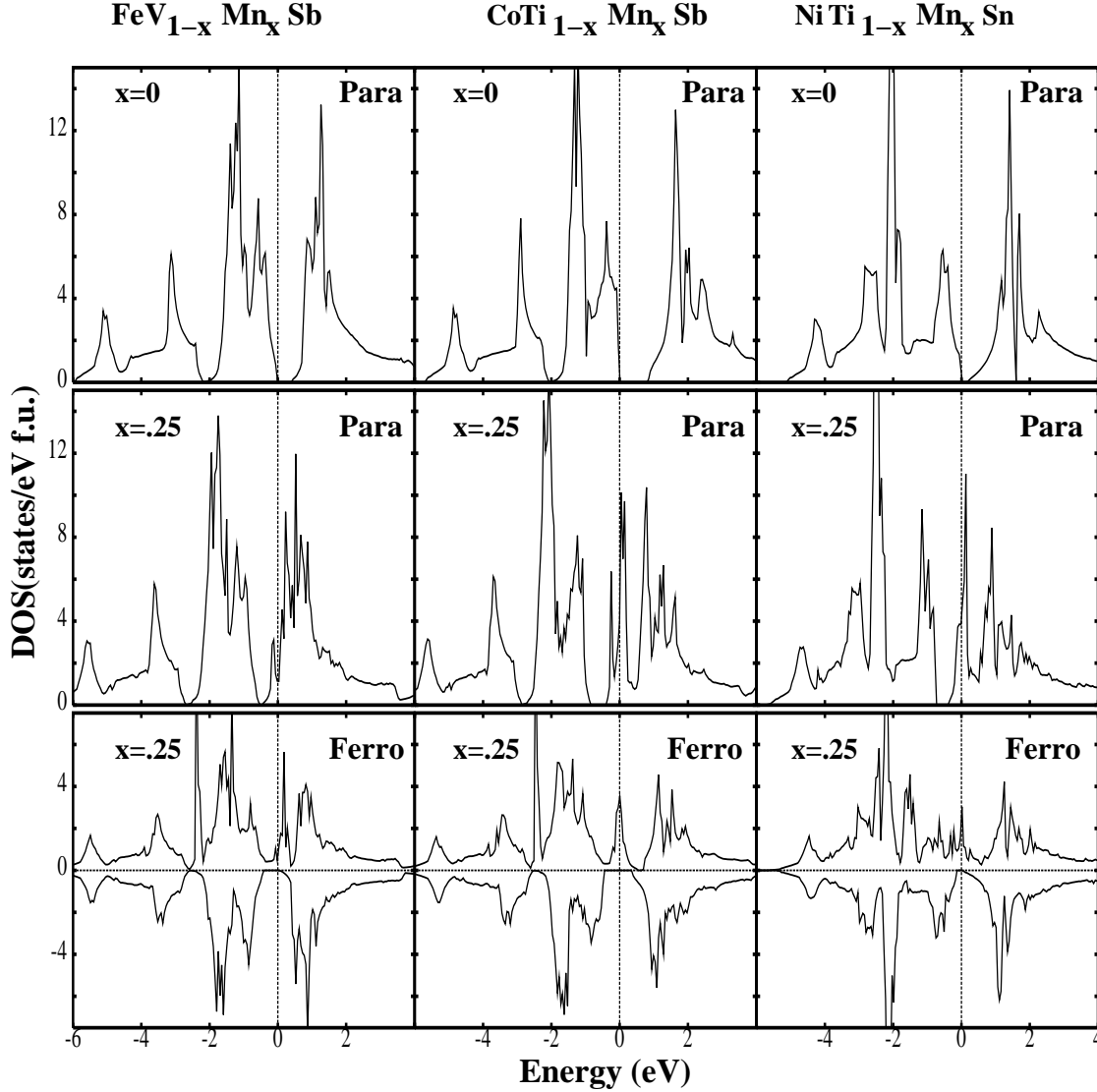


Figure 2. Density of states for formula unit for $\text{FeV}_{1-x}\text{Mn}_x\text{Sb}$ (first panel), $\text{CoTi}_{1-x}\text{Mn}_x\text{Sb}$ (second panel) and $\text{NiTi}_{1-x}\text{Mn}_x\text{Sn}$ (third panel). The first row shows the paramagnetic density of states of the semiconducting compound ($x=0.0$). Second and third row respectively show the paramagnetic and ferromagnetic density of states of the Mn doped compound ($x=0.25$). All energies are w.r.t. Fermi energy.

atomic spheres remains within the permissible limit of the ASA. The basis set of the self-consistent electronic structure calculation includes X,Y,M (s,p,d) and Z(s,p) and the rest are downfolded. A $[16,16,16]$ k-mesh has been used for self-consistency for all the calculations except for largest supercell where we have used $[8,8,8]$ k-mesh. All the k-space integration was performed using the tetrahedron method[29]. Experimental lattice parameters 5.82\AA , 5.88\AA [19], 5.924\AA [30] for FeVSb, CoTiSb and NiTiSn respectively were used for the doped structure and structural relaxations around the impurities were not included in the present calculations.

3. Results and discussions

3.1. Paramagnetic electronic structure of $XM_xY_{1-x}Z$

In this section, we shall present the results of the TB-LMTO-ASA electronic structure calculations for the Mn doped semiconducting half-Heusler systems in the unstable paramagnetic phase. We have considered three narrow gap semiconducting half-Heusler systems, FeVSb, CoTiSb and NiTiSn as the host material. In each system the lower valent transition element (V and Ti) is substituted with M (Mn,Cr) with concentration ranging from 25% to 3.125%. Our calculations[31] suggest that M substitution at other sites namely X(Fe,Co,Ni), Z(Sn,Sb) and the voids is energetically unfavorable. This result is consistent with a recent KKR-CPA calculations on some of these systems[20]. In first and second rows of figure 2 first and second row we have displayed the total density of states(DOS) for the semiconducting half-Heusler hosts and the doped systems $XMn_{0.25}Y_{0.75}Z$ in the paramagnetic phase respectively. Before we discuss the electronic structure of the doped systems we shall briefly discuss the electronic structure of the host materials.

The characteristic feature of the electronic structure of the undoped compounds (XYZ, VEC=18, semiconducting) shown in the first row of figure 2 is a pair of bonding and antibonding states separated by a gap. The bonding states below the gap are predominantly of X character while the antibonding states are of Y character. The semiconducting gap is a consequence of the covalent hybridization of the higher valent transition element X with the lower valent transition element Y. Further the bonding states are well separated from the Sb-p states in FeVSb and CoTiSb by a small pd gap, while the Sb-s states are lying far below the chosen scale of the figure. In NiTiSn, the Sn p states lies higher in energy compared to Sb, overlapping with the bonding complex and therefore the p-d gap does not exist. Again the Sn-s states are far below the chosen scale of the figure. So below the d-d gap there are 9 bands (4 Z s+p, and 5 predominantly X-d) which in the paramagnetic phase can accommodate 18 electrons of both spins. Hence with 18 valence electrons all the s-p and d states below the d-d gap are saturated resulting in bond-orbitals with strong directionality and bonding. This explains why half-Heusler systems with 18 valence electrons are semiconductors[25, 32]. We note that the presence of the Z(Sb/Sn) atom which provides a channel to accommodate some transition metal d electrons in addition to its sp electron is therefore crucial for the stability of these systems. For the half-Heusler systems with more than 18 valence electrons the antibonding states are occupied, and if the DOS at the Fermi level is high then the paramagnetic state is no longer stable and the stability can be achieved by developing a magnetic order. We have recently shown[25] that the presence of a gap in the paramagnetic phase promotes half-metallic ferromagnetism for systems with VEC > 18 as for *e.g.* realized in NiMnSb.

We shall now consider the doped systems in the paramagnetic phase shown in the second row of figure 2. In the doped systems replacing Ti/V with Mn puts an additional three/two electron in the system per Mn (VEC > 18), as a consequence the

systems are no longer semiconducting. This is reflected in the DOS for 25% Mn doped compound as a deep donor level produced by the addition of Mn impurities and the Fermi level lies on this predominantly Mn driven state. It is clear from the DOS peaks, that the paramagnetic phase has a Stoner instability and a ferromagnetic state with finite moment is likely to be energetically favorable to the paramagnetic state. The calculated DOS at the Fermi level $D(E_F)$ is 2.21, 6.2 and 7.5 states/eV/Mn for 25 % Mn-doped FeVSb, CoTiSb and NiTiSn respectively. Assuming the usual value of the Stoner interaction parameter $I_{Mn}=0.75\text{eV}$ leads to $D(E_f)I \simeq 1.7, 4.6, 5.6$, suggesting Stoner instability, particularly strong for Mn doped NiTiSn and considerable energy gain via spin polarization.

3.2. Spin-polarized Calculations

Figure 2 (third row) displays the spin-polarized DOS for the 25% Mn doped compound in the semiconducting host. From the figure we gather that the doped systems are not only ferromagnetic but also half-metallic sustaining an integral moment of $3 \mu_B$ for Mn in NiTiSn, CoTiSb and $2 \mu_B$ in FeVSb(see table 1). Interestingly the defect states are screened metallicly by the majority states so that the number of minority states do not change. The excess charge $\Delta z = 3, 3, 2$ per Mn in NiTiSn, CoTiSb and FeVSb respectively are accommodated in the majority spin channel, resulting in electronic states appearing as a new peak in the gap, which are primarily of Mn character. Hence the charge which is excess of $n \times 18$ (n = size of the supercell) appears as magnetic moment satisfying the 18 electron rule suggested for half-Heusler systems with $\text{VEC} > 18$ [32].

We shall now discuss in details the role of diluted magnetic impurities (Mn and Cr) in the three semiconducting hosts. In each case the lower-valent transition element Y has been replaced with $M(\text{Mn/Cr})\text{XM}_x\text{Y}_{1-x}\text{Z}$ with $x=12.5\%$, 6.25% , and 3.125% . For the purpose of discussion we have chosen a representative compound ($\text{NiTi}_{1-x}\text{Mn}_x\text{Sn}$), however our discussions holds for the other compounds as well. In figure 3 we have displayed the total DOS for one formula unit and the site projected Mn DOS for concentration $x = 12.5\%$, 6.25% , and 3.125% . We gather from the total DOS that all the systems are half-metallic ferromagnets. When Mn is substituted for Ti, the additional 3 electrons per Mn are accommodated in the majority spin channel producing a Mn-derived states in the gap while the minority states remain nearly unchanged. The width of the impurity states, which is a consequence of the hybridization with the transition elements(Ni,Ti) and Sn, decreases when the concentration of the impurity M is low. We also note that the Mn-derived states are partially filled. Further we gather from the Mn partial DOS, there are sharp Mn derived crystal field resonances deep in the valence band.

A Ti vacancy in NiTiSn creates holes in the Ni-d-Sn-p valence band hybrid due to depletion of four electrons per Ti, leaving the Ni-d Sn-p dangling bonds unsaturated. When Mn having seven valence electrons is substituted, four electrons are utilized to saturate the dangling bonds and the additional three electrons , responsible for the

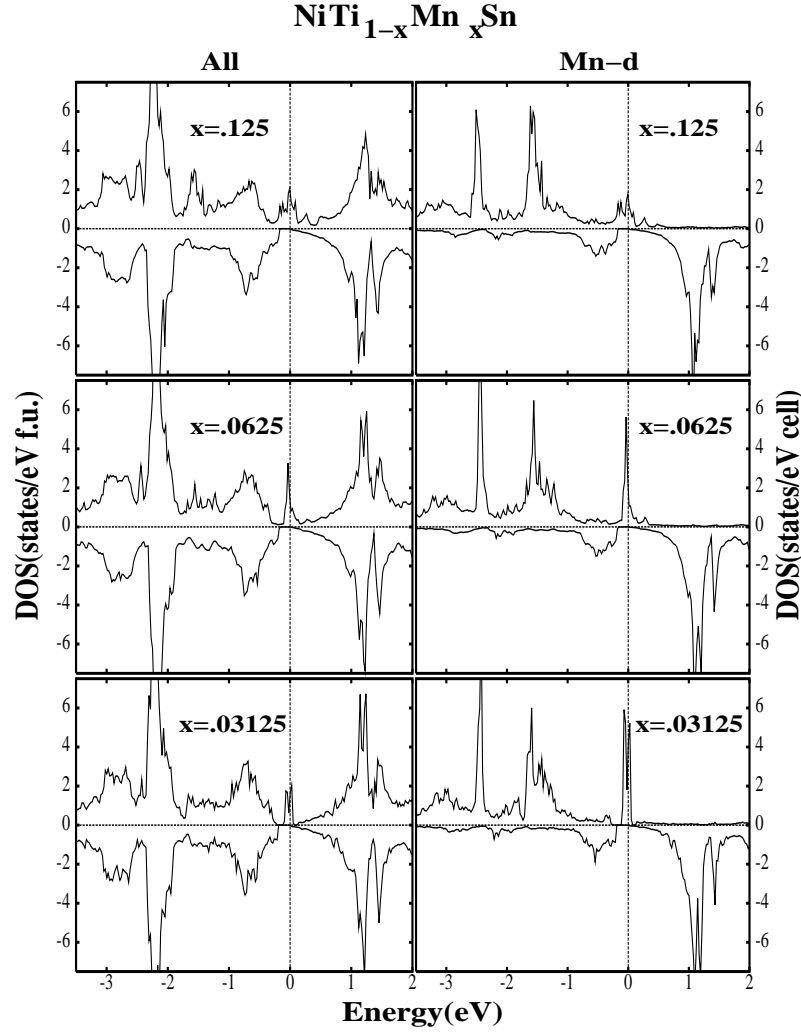


Figure 3. Spin-polarized density of states for $\text{NiTi}_{1-x}\text{Mn}_x\text{Sn}$ ($x=12.5\%$, 6.25% , 3.125%). In the left column total density of states per formula unit are plotted while in the right column the Mn-d states per cell are plotted. All energies are w.r.t. Fermi energy.

magnetic properties are accommodated in the high spin-state in the majority spin channel. This distribution of the Mn electrons results in crystal field resonances deep in the valence band, in addition to the partially filled impurity-derived states in the gap in the majority spin channel.

The gross feature of the electronic structure and magnetism in transition metal doped semiconducting half-Heusler compounds can be understood by invoking a simple model, where we consider the interaction between the dopant transition metal M and the valence band X-Z hybrid. Our simple model is schematically sketched in figure 4. In view of the strong d-d interaction, the valence band hybrid to a first approximation is primarily of X-d character, which is split into t_{2g} and e_g levels by the crystal field. After acquiring transition metal M electrons it is full and weakly spin split as illustrated in

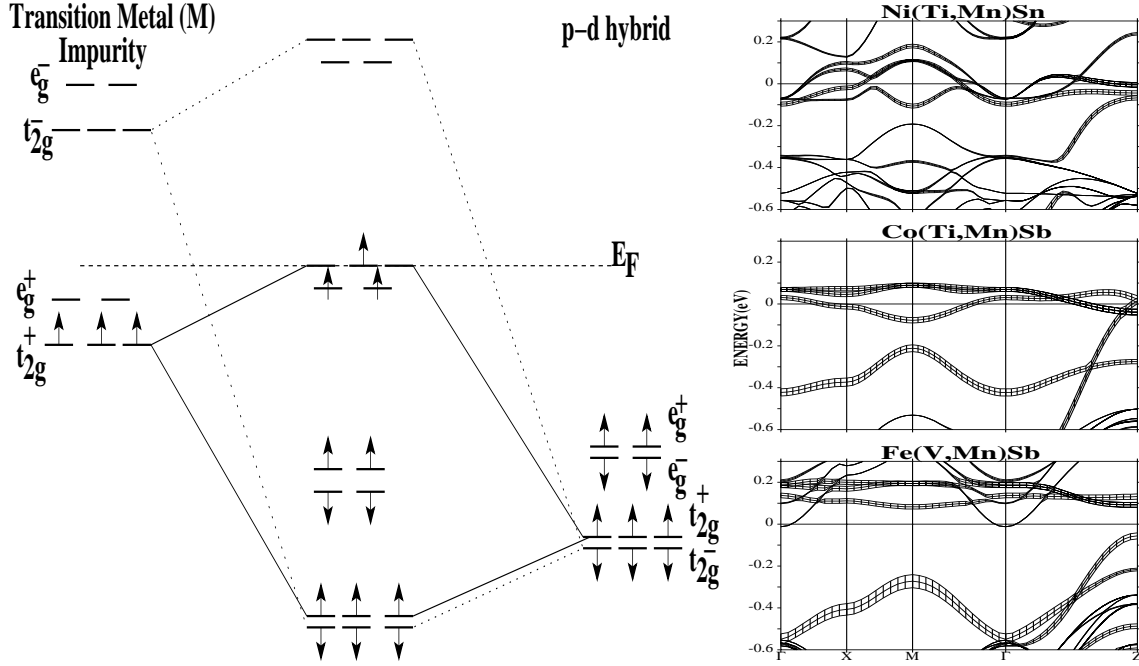


Figure 4. The gross feature of the electronic structure and genesis of magnetism is shown through a energy level diagram in the left and in the right the Mn-d characters (fat bands) are plotted for Ni(Ti,Mn)Sn, Co(Ti,Mn)Sb and Fe(V,Mn)Sb with 6.25% impurity concentrations. All energies are w.r.t. Fermi energy.

figure 4 (right panel). On the other hand the transition metal M-d levels are energetically shallower compared to the valence band hybrid. These levels are crystal field split as well as appreciably exchange split, as shown in figure 4 (left panel). The result in the presence of hybridization is shown in the central panel of the figure. Since the X atoms are arranged tetrahedrally to the M atoms strong X- t_{2g} -M- t_{2g} interaction is favored with relatively weaker e_g - e_g interaction. The up(+) and down(-) spin states on the transition metal atoms therefore interact via spin-conserving hopping interactions and form a set of bonding-antibonding states for each spin channel, as shown in the central panel of figure 4. We note from the central panel strong X- t_{2g} -M- t_{2g} hybridization places transition metal M- t_{2g} levels above the e_g levels, and the relative positions of these levels is governed by the strength of the X- t_{2g} -M- t_{2g} hybridization. We note from the M projected band structure(fat bands) shown in figure 4(right) that the bands close to the Fermi level are partially filled Mn-d bands as expected. We have recently shown[25] with the aid of a tight-binding analysis that this hybridization depends on the relative position of the transition elements X and M in the periodic table. As a consequence Fe-M hybridization > Co-M hybridization > Ni-M hybridization. This is further illustrated in figure 5, where we have displayed M (Mn/Cr) projected partial DOS in a narrow energy range about the Fermi level for $XM_xY_{1-x}Z$, with $x=6.25\%$ (only the spin up channel is shown as the spin down channel is empty in this energy range). We note from the figure that although the e_g and t_{2g} states are well split in Mn-doped

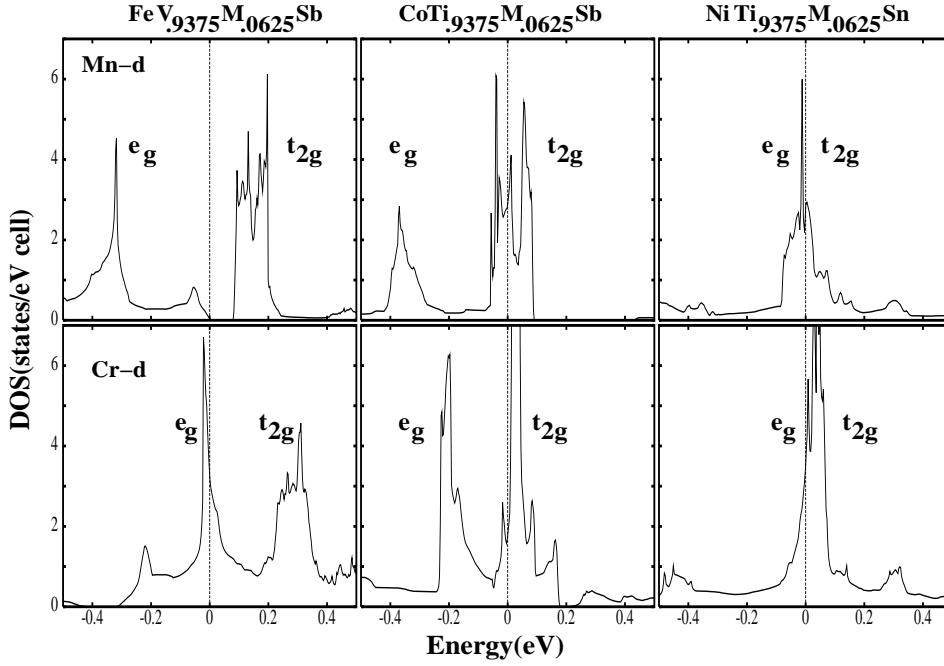


Figure 5. Spin-Up Mn-d(top) and Cr-d(bottom) density of states for the doped compounds with 6.25% concentration. All energies are w.r.t. Fermi energy.

FeVSb, the splitting decreases for CoTiSb, and is very small for Mn-doped NiTiSn, where the states are overlapping. So for Mn doped NiTiSn the additional three electrons progressively fill up the overlapping e_g and t_{2g} levels, with the t_{2g} partially empty. The same is true for Mn doped CoTiSb, while the e_g states are completely full for Mn-doped FeVSb (See figure 5). For the Cr doped systems the splitting is very small for all semiconducting hosts leaving the Cr-d states partially empty. The results of our calculations for the different hosts are summarized in table 1. We find from table 1 that the magnetic moment of M (Mn and Cr) remain almost the same with the concentration variation of M, with the only exception being Cr-doped FeVSb. This insensitivity of magnetic moment with concentration is a signature of localized d states of Mn and Cr. The localization comes from the fact that although d electrons of M are itinerant, the spin-down electrons are almost excluded from the M site. Further in all cases (except Cr-doped NiTiSn) the total moment is always integer, indicating a half-metallic solution.

Finally, we have addressed the issue of the tendencies towards ferromagnetic or antiferromagnetic ordering in these systems. For this purpose we have performed spin-polarized density functional calculations with (i) two M spins parallel to each other, the ferromagnetic configuration, (ii) two M spins anti-parallel to each other, the antiferromagnetic configuration. In order to understand the trends we have considered the hosts NiTiSn, CoTiSb and FeVSb doped with Mn and our results are summarized in table 2.

The stability of such a configuration in the context of diluted magnetic

Table 1. Magnetic moments in μ_B of doped half-Heusler compounds

Host compound	Impurity M	Impurity Conc. in %	Total Mag.Mom.	M Mag.Mom.	p-d hybrid (X+Z) Mag.Mom.	Y+E Mag.Mom.
FeVSb	Mn	25.00	2.00	2.67	-0.98	0.31
		12.50	2.00	2.64	-1.15	0.51
		6.250	2.00	2.61	-1.34	0.73
		3.125	2.00	2.58	-1.45	0.87
CoTiSb		25.00	3.00	3.25	0.05	-0.30
		12.50	3.00	3.24	-0.05	-0.19
		6.250	3.00	3.24	-0.16	-0.08
		3.125	3.00	3.22	-0.27	0.05
NiTiSn		25.00	3.00	3.44	0.04	-0.48
		12.50	3.00	3.41	0.07	-0.48
		6.250	3.00	3.43	0.06	-0.49
		3.125	3.00	3.40	0.01	-0.41
FeVSb	Cr	25.00	1.00	1.68	-0.95	0.27
		12.50	1.00	1.54	-1.02	0.48
		6.250	1.00	1.37	-1.12	0.75
CoTiSb		25.00	2.00	2.58	-0.49	-0.09
		12.50	2.00	2.53	-0.50	-0.03
		6.250	2.00	2.56	-0.69	0.13
NiTiSn		25.00	1.97	2.77	-0.25	-0.55
		12.50	1.85	2.64	-0.23	-0.56
		6.250	1.51	2.40	-0.25	-0.64

Table 2. Magnetic Moments in μ_B and $\Delta E(E_{FM}-E_{AFM})$ for double impurity

Host compound	Impurity Mn conc.	FM Total per Mn	FM Mn	AFM Total	AFM Mn	ΔE per Mn meV
FeVSb	25%	2.00	2.64	0.00	2.65	-71.4
	12.5%	2.00	2.60	0.00	2.57	-39.2
	6.25%	2.00	2.56	0.00	2.56	-12.8
CoTiSb	25%	3.00	3.22	0.00	3.28	-283.1
	12.5%	3.00	3.21	0.00	3.22	-140.9
	6.25%	3.00	3.21	0.00	3.16	-152.5
NiTiSn	25%	3.00	3.36	0.00	3.48	-282.9
	12.5%	3.00	3.36	0.00	3.43	-179.3
	6.25%	3.00	3.32	0.00	3.38	-243.0

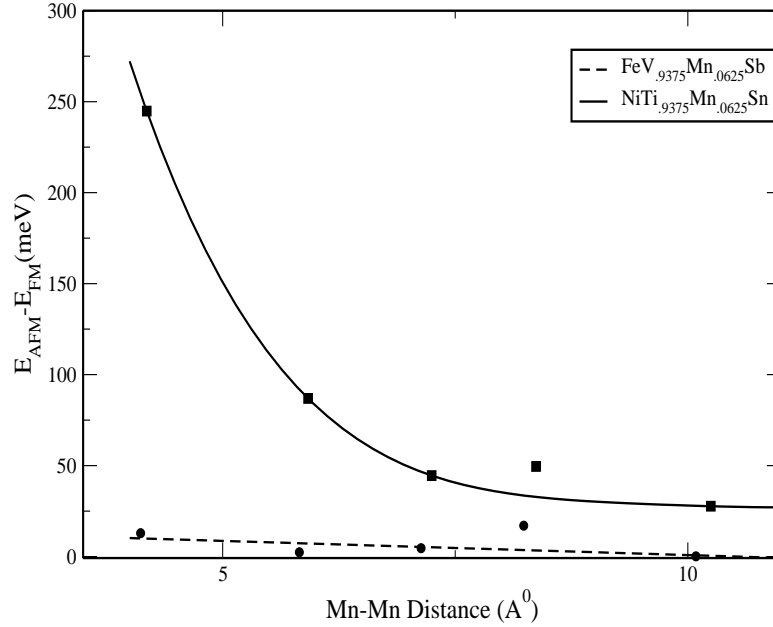


Figure 6. Energy difference between the AFM and FM phase ΔE ($= E_{AFM} - E_{FM}$ w.r.t the Mn-Mn distance for $\text{FeV}_{.9375}\text{Mn}_{.0625}\text{Sb}$ and $\text{NiTi}_{.9375}\text{Mn}_{.0625}\text{Sn}$.

semiconductors is usually discussed in the framework of Anderson-Hasegawa model[33]. If the M 3d orbital is partially occupied, in that case the 3d electrons in the partially occupied M orbitals are allowed to hop to the neighboring M 3-d orbitals, provided that the neighboring M ions have parallel magnetic moments. As a result, the d electrons lowers its kinetic energy by hopping in the ferromagnetic state. This is the so called double exchange mechanism. However if the transition-metal M d orbitals are full then this reduction via hopping is not possible, and the energy is lowered by super-exchange which requires the neighboring spins to be anti-parallel. In view of this it is expected that Mn-doped NiTiSn with partially occupied d levels should be ferromagnetic while Mn-doped FeVSb with empty t_{2g} orbitals should favor antiferromagnetic arrangement of spins. The total energy difference between FM and AFM configuration displayed in the last column of table 2 favors strong ferromagnetism for Mn doped NiTiSn and CoTiSb and is consistent with the Anderson-Hasegawa model, while for Mn doped FeVSb instead of expected AFM, ferromagnetic state is found to be stable although the energy difference ΔE is very small. For the cases where the e_g and t_{2g} states are nearly overlapping and the number of d electrons is less than five so that the d-manifold is only partially occupied, ferromagnetism is always stabilized. Finally, in figure 6 we have plotted ΔE as a function of Mn-Mn separation in the unit cell for Mn doped FeVSb and NiTiSn. This difference in energy ΔE is also a measure of interatomic exchange interaction, and in the framework of mean-field theory is also proportional to T_c . Although ΔE is positive for both cases however it is very small for Mn doped FeVSb, suggestive of the fact that ferromagnetism may not be sustained in this compound. This is consistent with the Anderson-Hasegawa model. Appreciable

ΔE for Mn doped NiTiSn suggests not only ferromagnetism for this compound but also appreciable T_c . Further, ΔE decreases sharply with distance suggesting that the double exchange mediated ferromagnetic interaction in these systems is short ranged. A Similar finding has been reported for Mn doped GaN[34], where it has been suggested short range interactions indicates the formation of Mn clusters within a short radial distance and might lead to high value of T_c in these systems.

4. Summary and Conclusions

We have studied in details the electronic structure and magnetism in Mn- and Cr-doped semiconducting half-Heusler systems, namely FeVSb, CoTiSb and NiTiSn, for a wide concentration range. The characteristic feature of the electronic structure is a deep defect state of predominantly Mn/Cr character, in the majority spin channel. The ferromagnetism in this systems can be understood within Anderson-Haswagawa model, which promotes ferromagnetism for partially filled d states. The electronic structure of the doped systems is analyzed in the framework of a simple model where we have considered the interaction between the dopant transition metal M and the valence band X-Z hybrid. We have shown that strong X- t_{2g} and M- t_{2g} interactions places the M -d sates close to the Fermi level, with the t_{2g} states lying higher in energy in comparison to the e_g sates. Further the splitting of the d levels is not only governed by the local crystal field but also on the strength of hybridization between X- t_{2g} and M- t_{2g} sates. Depending on the number of available d-electrons, ferromagnetism is realized provided the d-manifold is partially empty, as suggested by the Anderson-Hasegawa model. We have also addressed the issue of the tendencies toward ferromagnetic or antiferromagnetic ordering in these systems. Our calculations suggest that the double exchange mediated ferromagnetism in these systems is short ranged. Further the strong preference for ferromagnetic ordering over antiferromagnetic ordering in Mn-doped NiTiSn indicates it to be half-metallic ferromagnet with possibly high Curie temperature. Based on these theoretical predictions it will be interesting to investigate these systems experimentally.

Acknowledgments

We thank S.D. Mahanti for useful discussions. BRKN thanks CSIR, India, for research fellowship(SRF). The research is funded by CSIR (No. 03(0931)/01/EMR-II)

References

- [1] Ohno H, 1998 Science **281** 951
- [2] Theodoropoulou N and Hebard A F 2003 **89** 107203
- [3] Medvedkin G A, Ishibashi T, Nishi T, Hayata K, Hasegawa Y and Sato K 2000 Jpn. J. Appl. Phys. **39** L949
- [4] Theodoropoulou N, Hebard A F, Overberg M E, Abernathy C R, Pearton S J, Chu S N G and Wilson R G 2001 Appl. Phys. Lett. **78** 3475

- [5] Reed M L, El-Masry N A, Stadelmaier H H, Ritums M K, Reed M J, Parker C A, Roberts J C and Bedair S M 2001 Appl. Phys. Lett. **79** 3473
- [6] Matsumoto Y, Murakami M, Shono T, Hasagawa T, Fukumura T, Kawasaki M, Ahmet P, Chikyow T, Koshihara S and Koinuma H 2001 Science **291** 854
- [7] Ogale S B, Choudhary R J, Buban J P, Lofland S E, Shinde S R, Kale S N, Kulkarni V N, Higgins J, Lanci C, Simpson J R, Browning N D, Das Sarma S, Drew H D, Greene R L and Venkatesan T 2003 Phys. Rev. Lett. **91** 077205
- [8] Zhao Y G, Shinde S R, Ogale S B, Higgins J, Choudhary R J, Kulkarni V N, Greene R L, Venkatesan T, Lofland S E, Lanci C, Buban J P, Browning N D, Das Sarma S and Millis A J 2003 App. Phys. Lett. **83** 2199
- [9] Matsukura F, Ohno H, Shen A and Sugawara Y 1998 Phys. Rev. B **57** R2037; Dietl T, Ohno H, Matsukura F, Cibert J and Ferrand C 2000 Science **287** 1019; Konig J, Lin H-H and MacDonald A H 2000 Phys. Rev. Lett. **84** 5628
- [10] Dietl T, Ohno H, Matsukura F, Cibert J and Ferrand C 2000 Science **287** 1019
- [11] Sato K, Dederichs P H, Katayama-Yoshida H and Kudrnovsky J 2003 Physica B **340-342** 863; 2004 J. Phys. Condens. Matter **16** S5491; Mahadevan P and Zunger A 2003 Phys. Rev. B **68** 075202
- [12] Sarma D D 2001 Current Opinion in Solid State and Mat. Sc. **5** 261; Sarma D D, Mahadevan P, Saha-Dasgupta T, Ray S and Kumar A 2000 Phys. Rev. Lett. **85** 2549
- [13] Akai H 1998 Phys. Rev. Lett. **81** 3002; Schilfgaarde M van and Mryasov O N 2001 Phys. Rev. B **63** 233205
- [14] Dyck J S, Hajek P, Lostak P and Uher C 2002 Phys. Rev. B **65** 115212
- [15] Miao M S and Lambrecht W R L 2003 Phys. Rev. B **68** 125204
- [16] Forster R H, Johnston G B and Wheeler D A 1968 J. Phys. Chem. Solids **29** 855
- [17] De Groot R A, Muller F M, Van Engen P G and Buschow K H J 1983 Phys. Rev. Lett. **50** 2024
- [18] Xia Y, Bhattacharya S, Ponnambalm V, Pope A L, Poon S J and Tritt T M 2000 J. App. Phys. **88** 1952
- [19] Evers C B H, Richter C G, Hartjes K and Jeitschko W 1997 J. Alloys Compounds **252** 93
- [20] Tobola J, Kaprzyk S and Pecher P 2003 Phys. Status Solidi(b) **236** 531
- [21] van Leuken H and de Groot R A 1995 Phys. Rev. Lett. **74** 1171
- [22] Andersen O K and Jepsen O 1984 Phys. Rev. Lett. **53** 2571; Jepsen O and Andersen O K 2000 The Stuttgart TB-LMTO-ASA program, version 47
- [23] Andersen O K, Pawlowska Z and Jepsen O 1986, Phys. Rev. B **34** 5253
- [24] Pawlowska Z, Christensen N E, Satpathy S and Jepsen O 1986 Phys. Rev. B **34** 7080
- [25] Nanda B R K and Dasgupta I 2003 J. Phys. Condens. Mat. **15** 7307; Nanda B.R.K and Dasgupta I 2005 Comp. Mat. Sc. 2006 **36** 96
- [26] Dronskowski R and Blochl P E 1993, J. Phys Chem **97** 8617
- [27] Von Barth U 1972 J. Phys. C: Solid State Phys. **5** 1629; Hedin L 1971 J. Phys. Solid State Phys. **4** 2064
- [28] Perdew J P, Burke K and Ernzerhof M 1996 Phys. Rev. Lett. **77** 3865
- [29] Jepsen O and Andersen O K 1971 Solid State Commun. **9** 1763; Blochl P, Jepsen O and Andersen O K 1994 Phys. Rev. B **49** 16223
- [30] Aliev F G, Brandt N B, Moschalkov V V, Kozyrkov V V, Scolozdra V V and Belogorokhov A I 1990 Z. Phys. B **80** 353
- [31] Nanda B R K and Dasgupta I *unpublished*
- [32] Galankis I, Dederichs P H and Papanikolaou N 2002 Phys. Rev. B **66** 134428
- [33] Anderson P W and Hasegawa H, 1955 Phys. Rev. **100** 675
- [34] Sanyal B, Bengone O and Mirbt S 2003 Phys. Rev. B **68** 205210